Optical Spectroscopic Study of the Effects of a Single Deoxyribose Substitution in a Ribose Backbone: Implications in RNA−RNA Interaction†

Martina Lindqvist,‡ Munna Sarkar,*,§ Anna Winqvist,|| Eriks Rozners,|| Roger Strömberg,|| and Astrid Gräslund*,‡

Department of Biophysics, Arrhenius Laboratories, Stockholm University, S-10691 Stockholm, Sweden, Nuclear Chemistry Division, Saha Institute of Nuclear Physics, 1/AF, Bidhannagar, Calcutta-700064, India, and Laboratory of Organic and Bioorganic Chemistry, Department of Medical Biochemistry and Biophysics, Karolinska Institute, S-17177 Stockholm, Sweden

Received September 1, 1999; Revised Manuscript Received December 3, 1999

ABSTRACT: The 2′-OH group in the ribose sugars of an RNA molecule plays an important role in guiding tertiary interactions that stabilize different RNA structural motifs. Deoxyribose, or 2′-OH by 2′-H, substitution in both the single-stranded and the duplex part of an RNA backbone has been routinely used to evaluate what role the 2′-OH plays in different tertiary interactions that guide an RNA−RNA contact. A deoxyribose substitution not only has the effect of removing a hydrogen bond donating group, but also introduces a sugar moiety with a preference for C2′-endo pucker in a backbone of predominantly C3′-endo sugars. This study evaluates the effects of a single deoxyribose substitution in both single-stranded and double-helical forms of RNA oligomers. A single-stranded, nonrepetitive 7-mer oligoribonucleotide (7-mer RNA) and four different variants having the same base sequence but with a single deoxyribose sugar at different positions in the strands have been studied by ultraviolet (UV) absorption, circular dichroism (CD), and Fourier transform infrared (FTIR) spectroscopy. Duplexes were formed by association with the complementary strand of the 7-mer RNA. The results show that both RNA and DNA single strands have preorganized conformations with spectral properties resembling those of A- and B-form helices, respectively, with RNA being more heterogeneous than its DNA counterpart. A single deoxyribose substitution perturbs the structure of the RNA backbone, with the effect being more pronounced in the single-stranded than in the duplex structure. The perturbation depends on the position of the 2′-H substitution in the strand.

The essential difference in the sugar−phosphate backbone between RNA[1] and DNA is the presence of the 2′-hydroxyl groups in the ribose sugars that can act as hydrogen bond donors. These 2′-OH groups play a dominant role in modulating the hydration pattern in RNA molecules (*1, 2*), that in turn determine the flexibility of RNA structures (*2*). The 2′-OH in the RNA backbone also fine-tunes the different stereo-electronic effects that guide the sugar pucker (*3, 4*). The sugar conformations in an RNA molecule depend to a large extent upon interactions with the local environment guided by forces such as hydrogen bonding, changes in sugar−phosphate backbone torsion, and base stacking interactions. Even though RNA duplexes are frequently found to have C3′-endo conformation or N-type sugar pucker, S-type sugars with C2′-endo conformation are also found in single-stranded regions of some RNA hairpin loops (*5*).

Interactions between RNA molecules may be based on sequence recognition in which two RNA molecules form base pairs, and/or structural recognition involving tertiary interactions between RNA motifs. Tertiary interactions between different structural domains of catalytic RNA molecules guide the folding of their three-dimensional structures into their active conformations, and are also necessary for stabilization of the enzyme−substrate complex of ribozymes. Many of these interactions involve the participation of the ribose 2′-OH groups which are involved in various intra- and intermolecular interactions with chemical groups in nearby nucleotides, either through direct hydrogen bonding or mediated by water bridges (*1, 6*). The availability of chemical groups for hydrogen bonding will depend on the local stereochemical arrangement of the groups with respect to the 2′-OH of a ribose, which in turn will depend on the sugar pucker at that particular 2′-OH position. Replacement of a ribose sugar by deoxyribose (2′-OH→2′-H) in an RNA backbone not only removes a hydrogen bond donating group in that sugar moiety, but also introduces a sugar with a preference for S-type puckering.

The effect of having ribose sugars in a predominantly deoxyribose backbone has been studied in chimeric RNA−DNA oligomers (*6*). The presence of a single 2′-OH group in the sugar−phosphate backbone of a B-DNA decamer duplex induced A-form helical conformation of the entire

† This study was supported by grants from the Swedish Natural Science Research Council, the Swedish Research Council for Engineering Sciences, and the Foundation of Strategic Research in Sweden.

* To whom correspondence should be addressed. All correspondence should be addressed to the Department of Biophysics, Arrhenius Laboratories, Stockholm University, S-10691 Stockholm, Sweden.

‡ Stockholm University.

§ Saha Institute of Nuclear Physics.

|| Karolinska Institute.

[1] Abbreviations: UV, ultraviolet absorption spectroscopy; CD, circular dichroism spectroscopy; FTIR, Fourier transform infrared spectroscopy; RNA, ribonucleic acid; DNA, deoxyribonucleic acid.

10.1021/bi992055n CCC: $19.00
Published on Web 01/29/2000

duplex (*7*). The presence of two ribose sugars at each end of a DNA duplex or two ribose sugars near the center of a DNA duplex induce A-helical conformation in the duplexes as seen in their crystal structures (*8*). However, the structures of these chimeras deviate from a regular A-geometry, and their conformations depended on the position of ribose substitution in the duplexes. Heterogeneous sugar puckers other than N- and S-types were found not only at the ribose−deoxyribose junctions but also away from them.

2′-H substitution in both single-stranded and the duplex part of an RNA backbone has been routinely used to evaluate what role the 2′-OH groups play in different ribozyme tertiary interactions (*9*−*16*). A single 2′-H substitution in the active core of a ribozyme derived from a group I intron has been shown to have strong deleterious effect on catalysis (*17*). This single deoxyribose substitution was made in the 'triple helical' domain of that ribozyme. The triple helical domain is an RNA structural motif in the catalytic core of a self-splicing group I intron, which is formed by nucleoside triple interactions of single-stranded regions J6/7 and J3/4 in the major and minor grooves of P4 helix and P6 helices, respectively. It is a crucial motif required for the correct orientation of the helices in the three-dimensional structure of the intron (*18*).

To be able to understand the different factors guiding recognition and formation of RNA−RNA contacts, it is important to know the effects of a deoxyribose sugar substitution in an RNA backbone. Is it only a removal of one hydrogen bond donating group, or does the introduction of a sugar with a preference for S-type puckering in a backbone of predominantly N-type of sugars have a significant effect in perturbing the local geometry?

To answer this question, we have studied a single-stranded 7-mer RNA having the same base sequence as the J6/7 and 3′-end bases of the P6 helix of a self-splicing group I intron (Figure 1a, i). This 7-mer RNA has been shown by us to associate with a 23-mer RNA in the presence of Mg^{2+} to model the interactions in the triple helical domain of a self-splicing group I intron from bacteriophage T4 *nrdB* pre-mRNA (*19*). Association was inhibited when only one deoxyribose sugar was substituted at a crucial position in the 7-mer RNA single strand as in ssdG451 and ssdU453 (*20*) (Figure 1a, ii and iv). This implies that a single deoxyribose sugar is sufficient to perturb RNA−RNA interactions that guide the formation of the triple helical domain. We have synthesized four different variants of the 7-mer RNA (ssdG451, ssdU452, ssdU453, and ssdC454; Figure 1a, ii−v), with identical base sequence but each having a single deoxyribose sugar at a particular position in the single strand. The nucleotide numbers used in the text correspond to those in the original group I intron sequence. We have further extended our studies to duplexes formed with the complementary strand of the 7-mer RNA, to see whether the perturbing effects of a single 2′-H substitution would increase or decrease when put into a more defined structure of a duplex. For comparison, we also studied the equivalent 7-mer DNA and 7-mer DNA duplex having the same base sequence as the corresponding 7-mer RNAs, except with T replacing U in the DNA strands. The techniques used were ultraviolet (UV) absorption, circular dichroism (CD), and Fourier transform infrared (FTIR) spectroscopy.

MATERIALS AND METHODS

Synthesis of Oligonucleotides. The oligoribonucleotides (7-mer RNA and 7-mer RNA complementary strand) and the single deoxyribose substituted 7-mer RNA variants (ssdG451, ssdU452, ssdU453, and ssdC454) were prepared with the H-phosphonate method as described (*19*, *21*) except that a polystyrene solid support (*22*) was used and the HPLC purification was instead done as follows: first by ion exchange chromatography on a semipreparative Dionex NucleoPac PA-100 column using a flow rate of 3 mL/min and a linear gradient of 0−120 mM lithium perchlorate in 20 mM aqueous sodium acetate containing 10% acetonitrile (pH 6.5) during 45 min. The collected fractions were lyophilized, and the residues were dissolved in 0.1 M aqueous triethylammonium acetate (1 mL) and further purified by reversed phase HPLC on a Hypersil ODS 5 μm column using a flow rate of 1 mL/min and a linear gradient of 0−25% acetonitrile in 0.1 M aqueous triethylammonium acetate (pH 6.5) during 40 min. The collected fractions were lyophilized, and subsequent removal of remaining triethylammonium acetate was performed by redissolving the oligonucleotides in distilled water (5 mL) and lyophilizing the solutions; the procedure was repeated 3 times.

The oligodeoxyribonucleotides (7-mer DNA and 7-mer DNA complementary strand) were obtained from Kebo Lab, Stockholm, Sweden.

Sample Preparation. Stock solutions of single strands were prepared by directly dissolving dry and desalted oligomers into double-distilled sterilized water. Concentrations were determined spectrophotometrically at 260 nm and 25 °C, using extinction coefficients for single strands calculated by nearest-neighbor analysis (*23*): 7-mer RNA and all four 7-mer RNA variants (0.77×10^5 M^{-1} cm^{-1}); 7-mer RNA complementary strand (0.69×10^5 M^{-1} cm^{-1}); 7-mer DNA (0.74×10^5 M^{-1} cm^{-1}); 7-mer DNA complementary strand (0.66×10^5 M^{-1} cm^{-1}). Concentrations of stock solutions ranged between 1 and 9 mM in single strands. The final sample solutions were prepared using 10 mM sodium cacodylate buffer, 0.1 mM EDTA, pH 7.0. Sample concentrations for UV and CD experiments ranged between 10 and 20 μM in single strands, while the FTIR concentration was set to 10 mM in single strands. All samples contained 10 Mg^{2+}/single strand. The corresponding duplexes were formed by annealing the single-stranded 7-mer RNA or its different variants with the complementary strand of 7-mer RNA in a 1:1 stoichiometry. Duplex stock concentrations ranged between 1 and 3 mM in double strands, and the samples were prepared using the same buffer system as for the single strands. A concentration of approximately 40 μM in double strands was used for UV and CD experiments, while the FTIR concentration was set to 10 mM in double strands. All duplex samples contained 20 Mg^{2+}/duplex.

UV and CD Experiments. The UV melting profiles were obtained at 260 nm using a Cary 4 UV spectrophotometer equipped with a thermoregulator (Eurotherm 808) connected to an ethylene glycol water circulating bath (Lauda RM6). The temperature was continuously increased at an increment of 0.5 °C per minute. A quartz cuvette of 0.2 cm path length was used for the measurements. CD spectra were recorded on a Jasco 720 spectropolarimeter using the same samples as in the UV melting studies. The spectropolarimeter was

fitted with a thermoelectrically controlled cell holder, and experiments were performed at 4 °C. All measurements are the average of 9 scans.

FTIR Experiments. FTIR spectra were recorded at room temperature using a Perkin-Elmer Spectrum 2000 spectrometer equipped with a MIRTGS detector. Resolution was set to 2 cm^{-1}, 32 interferograms were recorded, and a strong Norton Beer apodization function was used for performing the Fourier transformation. Data processing was limited to multipoint baseline correction, where care was taken to achieve a smooth baseline with no abrupt nicks. In the case where an overlapping shoulder was present adjacent to a peak, the peak positions of the composite bands were determined by taking the second derivative of the baseline-corrected spectra. The second-derivative extreme points are not significantly affected by where baseline points are put in, giving band shifts only within the resolution (2 cm^{-1}). However, intensity ratios between bands within the same spectrum are very sensitive to what set of baseline points has been chosen, so to be able to compare band ratios obtained from one spectrum to that of another, the same set of baseline points were used for both spectra. The baseline points chosen in the two nonsubstituted RNA systems (the single- and double-stranded RNA, respectively) were used as a basic set of point positions for multipoint baseline correction for all the single-stranded and double-stranded RNA variants, whereupon only minor baseline point adjustments due to bandshifts had to be done.

FTIR spectra were recorded in both H_2O and D_2O using the same buffer system as mentioned above, with sample concentrations of 10 mM in single strands or double strands. The pD value for the D_2O solution is the pH value measured in the corresponding H_2O solution. Sample stock solutions, buffer, and $MgCl_2$ were deposited on demountable ZnSe windows in sets of maximum 2 μL droplets at a time. Between every addition, the solution was evaporated to dryness under a gentle flow of dry nitrogen. Finally, the dried sample was redissolved into 1 μL of H_2O or D_2O and sandwiched between the two ZnSe windows. The spectrometer sample chamber was continuously purged with dry air to remove water vapor. Each spectrum was measured several times with fresh samples to ensure the reproducibility of the spectral bands irrespective of any possible differences in sample handling.

RESULTS

UV and CD Spectroscopy. UV melting studies were carried out on single- and double-stranded oligomers (Figure 1), all having identical base sequence but with the position of the single deoxyribose sugar (2′-OH→2′-H) varying as indicated by the nucleotide numbers. UV experiments were performed in a 10 mM sodium cacodylate buffer containing 0.1 mM EDTA, pH 7.0, with a magnesium content of 10 Mg^{2+}/single strand and 20 Mg^{2+}/double strand. Hypochromicities were calculated using the formula: $[(A_{ss} - A_{ds})/A_{ss}] \times 100$ (%), where A_{ss} and A_{ds} are the single- and double-stranded absorbances, respectively. For the single-stranded oligomers, absorbances at 15 and 60 °C were used as A_{ds} and A_{ss}, respectively, while hypochromicities for double strands were calculated using absorbances A_{ds} and A_{ss} at temperatures as close as possible to the beginning and end of the helix-to-coil transition, respectively. The standard deviation was obtained from repeated measurements on three different preparations of the same sample. The hypochromicity values of the single strands (ss) (ss7RNA, ssdG451, ssdU452, ssdU453, ssdC454; see Figure 1) and double strands (ds) (ds7RNA, dsdG451, dsdU452, dsdU453, and dsdC454) only showed slight variations, varying between 3.1 ± 0.2% and 3.7 ± 0.3% for the single strands and between 13.2 ± 0.4% and 15.1 ± 0.5% for the double strands. As expected, the single strands have lower hypochromicity values due to less base stacking than their corresponding duplexes. Certain differences in melting point (T_m) values are seen for the duplexes. The ds7RNA shows maximum stability with a T_m of 38.6 ± 0.9 °C whereas the variant duplex dsdU452 shows a minimum thermal stability with a T_m of 34.4 ± 0.9 °C. All the other RNA variants also showed slightly less thermal stability as compared to ds7RNA.

a)	5′-A_{449}-G-G-U-U-C-A_{455}-3′	ss7RNA	**(i)**
	5′-A-G-**dG**$_{451}$-U-U-C-A-3′	ssdG451	**(ii)**
	5′-A-G-G-**dU**$_{452}$-U-C-A-3′	ssdU452	**(iii)**
	5′-A-G-G-U-**dU**$_{453}$-C-A-3′	ssdU453	**(iv)**
	5′-A-G-G-U-U-**dC**$_{454}$-A-3′	ssdC454	**(v)**
	5′-A-G-G-T-T-C-A-3′	ss7DNA	**(vi)**
b)	5′-A-G-G-U-U-C-A-3′ 3′-U-C-C-A-A-G-U-5′	ds7RNA	**(i)**
	5′-A-G-**dG**-U-U-C-A-3′ 3′-U-C - C-A-A-G-U-5′	dsdG451	**(ii)**
	5′-A-G-G-**dU**-U-C-A-3′ 3′-U-C-C - A-A-G-U-5′	dsdU452	**(iii)**
	5′-A-G-G-U-**dU**-C-A-3′ 3′-U-C-C-A - A-G-U-5′	dsdU453	**(iv)**
	5′-A-G-G-U-U-**dC**-A-3′ 3′-U-C-C-A-A - G-U-5′	dsdC454	**(v)**
	5′-A-G-G-T-T-C-A-3′ 3′-T-C-C-A-A-G-T-5′	ds7DNA	**(vi)**

FIGURE 1: (a) Single-stranded model sequences of (i) 7-mer RNA (nucleotides 449−455 in bacteriophage T4 *nrdB* pre-mRNA), (ii−v) different 7-mer variants (each named by the position of the deoxyribose-substituted nucleotide marked in boldface), and (vi) 7-mer DNA. (b) Double-stranded model sequences formed by addition of an all-RNA complementary strand to (i) 7-mer RNA and (ii−v) different 7-mer variants, and (vi) by addition of an all-DNA complementary strand to 7-mer DNA.

Figure 2a shows the overlaid CD spectra of all single-stranded 7-mers (RNA, DNA, and the four different variants). Even though the overall spectra of the RNA deoxy variants qualitatively agree more with the ss7RNA than with the ss7DNA, there are significant differences both to ss7RNA and also between the variants themselves. Figure 2b shows the overlaid CD spectra of the corresponding duplexes. Duplex RNA and all double-stranded variants show the overall features characteristic of an A-helix, with a large band around 245−300 nm and a large but narrower negative band with a peak at 211 nm (*24*, *25*), and appear to have more similarity in conformation than the single strands. The duplex DNA, on the other hand, shows the expected B-helix features, with a large positive peak at 280 nm and a negative band positioned around 242 nm (*24*, *25*).

FTIR Spectroscopy. FTIR spectroscopy is a sensitive technique to probe nucleic acid conformations. Infrared marker bands originating from vibrations of different chemi-

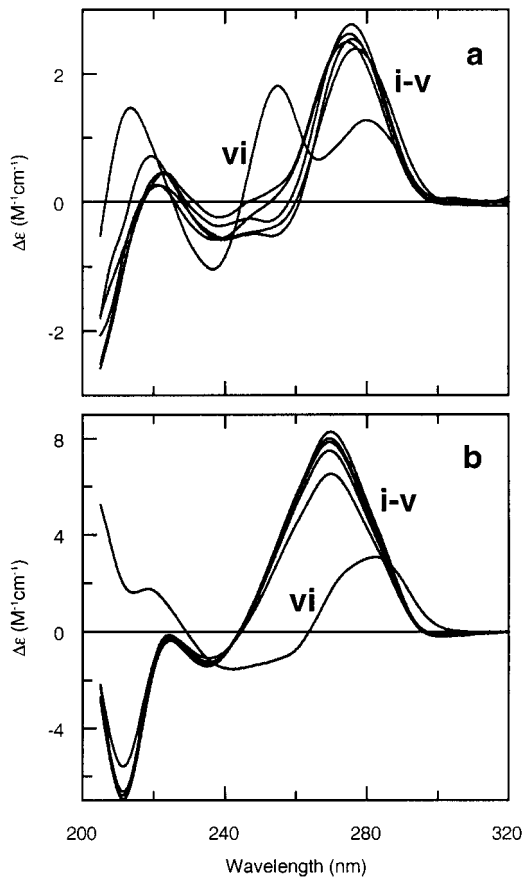

FIGURE 2: (a) CD spectra of single-stranded 7-mers: (i−v) RNA and different deoxyribose substituted variants; and (vi) DNA. (b) Double-stranded 7-mers: (i−v) RNA and different deoxyribose substituted variants; and (vi) DNA. Spectra recorded at 4 °C in 10 mM sodium cacodylate, 0.1 mM EDTA, pH 7.0, with a magnesium content of 10 Mg^{2+}/single strand and 20 Mg^{2+}/double strand. The CD results are presented on a per nucleotide basis.

cal groups in the bases, sugars, and phosphate backbone appear in different frequency regions in the FTIR spectra.

(a) Base Frequency Region (1800−1500 cm^{-1}). Figure 3a,b shows the FTIR spectra of the single and double strands in D_2O buffer in the 1760−1540 cm^{-1} region. Here absorption bands due to in-plane double bond base vibrations appear which are extremely sensitive to base stacking and base pairing interactions. A strong band dominates the FTIR spectra of single strands (Figure 3a) around 1690−1640 cm^{-1}, assigned to an overlapping contribution of C4═O4 of free, i.e., non-base-paired, uracils or thymines (for ss7DNA), C6═O6 of free guanines, and C2═O2 of free cytosines (*26*, *27*). The presence of this strong band show that the single strands are not in any associated form under the experimental conditions studied (*20*). In contrast, two bands dominate the FTIR spectra of the RNA duplex and its deoxy variants (Figure 3b): a band around 1684 cm^{-1} and a band around 1653 cm^{-1}. Whereas the former has been assigned to the C6═O6 of base paired guanines and C2═O2 bond stretching vibrations of uracils, the latter has been assigned to C2═O2 stretching vibrations of cytosines involved in base pairing (*20*, *26*, *28*). This verified that all the RNA double strands formed well-defined duplexes under the experimental conditions studied. The spectra of all RNA duplexes are very similar (Figure 3b). In the DNA duplex, the broad band around 1666 cm^{-1} involves contributions of C4═O4 of thymines and C2═O2 stretching vibrations of cytosines involved in base pairing (*26*, *28*). The band at 1646 cm^{-1} is due to the C═C, C═N ring vibrations of thymines engaged in base pairing (*29*).

The doublet in the region 1600−1550 cm^{-1} is assigned to the C═N stretching mode of guanines, whose position and intensity are sensitive to the environment of the guanine residues (*20*, *26*, *27*, *30*−*32*). In case of the single strands, this band is shifted from 1588 cm^{-1} for ss7RNA to 1579 cm^{-1} in ss7DNA (Figure 3a). This could indicate that the two guanines in the ss7RNA have quite different environments and/or stacking interactions as compared to that in ss7DNA. For all RNA deoxy variants, the single 2′-H substitution in the ribose backbone affects this guanine band, shifting it to lower wavenumber (1577 cm^{-1}). The shift occurs irrespective of whether the 2′-H substitution was done in a sugar attached to a guanine residue (ssdG451, Figure

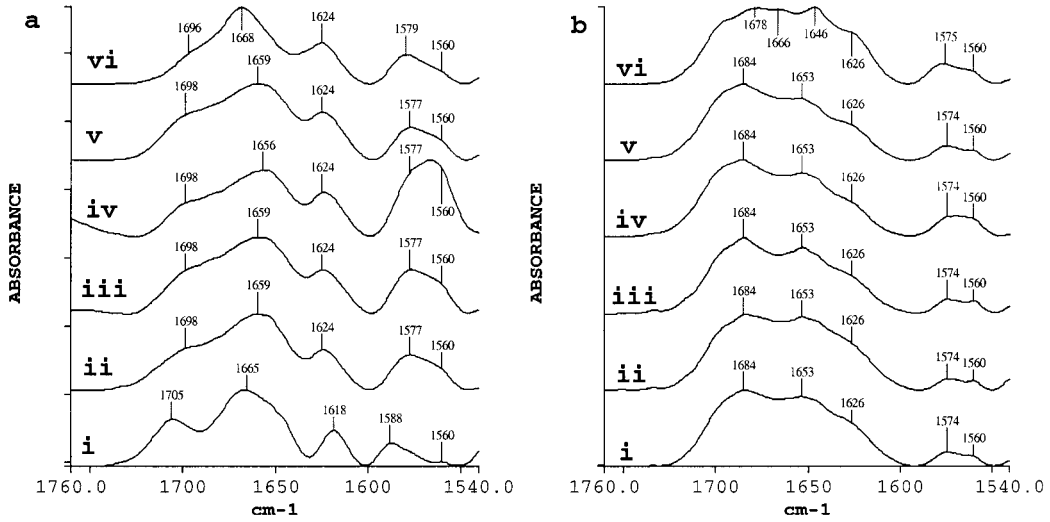

FIGURE 3: (a) Stacked FTIR spectra showing the 1760−1540 cm^{-1} region of single-stranded 7-mer sequences: (i) ss7RNA, (ii) ssdG451, (iii) ssdU452, (iv) ssdU453, (v) ssdC454, and (vi) ss7DNA. Concentrations set to 10 mM in single strands. (b) FTIR spectra of double-stranded 7-mer sequences: (i) ds7RNA, (ii) dsdG451, (iii) dsdU452, (iv) dsdU453, (v) dsdC454, and (vi) ds7DNA. Concentrations set to 10 mM in double strands. All spectra recorded in D_2O at room temperature in 10 mM sodium cacodylate, 0.1 mM EDTA, pH 7.0, with a magnesium content of 10 Mg^{2+}/single strand and 20 Mg^{2+}/double strand.

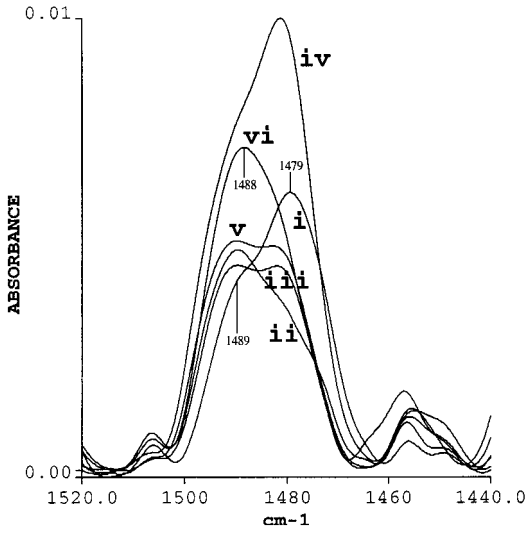

FIGURE 4: FTIR spectra showing the 1520−1440 cm^{-1} region of single-stranded 7-mer sequences: (i) ss7RNA, (ii) ssdG451, (iii) ssdU452, (iv) ssdU453, (v) ssdC454, and (vi) ss7DNA. Spectra recorded in H_2O at room temperature in 10 mM sodium cacodylate, 0.1 mM EDTA, pH 7.0, with a magnesium content of 10 Mg^{2+}/single strand.

1a, ii), or up to three nucleotides away from it (ssdC454, Figure 1a, v). In the case of the duplexes, the guanine C═N stretching vibration band appears in the region 1590−1550 cm^{-1}, with a peak at 1574 cm^{-1} and a shoulder around 1560 cm^{-1}. The position of this band is hardly affected by any of the single 2′-H substitutions (Figure 3b).

The spectra also show a band around 1700 cm^{-1} (Figure 3a) that is due to the C2═O2 stretch of non-base-paired uracils or thymines (*20*, *27*), and a band around 1625 cm^{-1} (Figure 3a,b) that is due to C═C and C═N ring vibrations of free or base paired adenines along with a minor contribution of some ring vibrations of free cytosines (*20*, *26*, *31*).

(b) Base−Sugar Frequency Region (1500−1250 cm^{-1}). In the region 1500−1250 cm^{-1}, marker bands for the base vibrations and base vibrations influenced by the sugar appear. The band around 1500−1470 cm^{-1} is assigned mainly to the imidazolic ring vibration of purines which depends strongly on the N7C8H bending vibrations (*33*−*36*). Any modification in the position of the band will reflect an interaction at the N7 sites. This band also has some overlapping contributions of ring vibrations of cytidines around 1496 cm^{-1} (*28*, *33*). Two bands are seen in the spectrum of ss7RNA and its deoxy variants (Figure 4). For ss7RNA, there is a shoulder around 1489 cm^{-1} and a peak at 1479 cm^{-1} (Figure 4, i). Making a deoxyribose substitution at G451 alters the ratio of the two bands such that a peak appears at 1489 cm^{-1} and a shoulder occurs at 1481 cm^{-1} (Figure 4, ii). The peak ratio changes significantly for the other deoxy variants, clearly dependent on the position of 2′-H substitution. In the case of single-stranded ss7DNA, there is a single broad peak in this region at 1488 cm^{-1} (Figure 4, vi). Overlapping contributions from additional cytidines present in the complementary strand (Figure 1b) make interpretation of this band in the duplex spectra more complicated.

(c) Backbone Frequency Region (1250−1000 cm^{-1}). Absorption bands arising from the phosphate backbone vibrations dominate the 1250−1000 cm^{-1} frequency region. The band in the region 1250−1200 cm^{-1} is a characteristic marker band for backbone conformation (*26*, *31*, *37*) and arises due to the antisymmetric PO_2^- stretching mode. This band is more sensitive to conformational changes between the A- and B-helical forms in the phosphate backbone than the symmetric PO_2^- stretching mode which appears around 1090−1080 cm^{-1}. The antisymmetric phosphate stretching vibrations are observed around 1245−1240 cm^{-1} for A-helices and near 1225 cm^{-1} for the B-family helices (*26*, *31*). For RNA molecules having some B-like character, an overlapping contribution from ribose vibrations around 1221 cm^{-1} makes the quantitative estimation of the B-like character in the RNA backbone a difficult task (*37*).

Figure 5 shows the antisymmetric phosphate stretching band for the single strands and duplexes. For the single-stranded 7-mer RNA (ss7RNA, Figure 5a, i), a peak around 1236 cm^{-1} and a shoulder around 1220 cm^{-1} are observed. In contrast, all RNA deoxy variants show a shoulder around 1238 cm^{-1} and a peak around 1218 cm^{-1}. The low wavenumber shift of the characteristic marker band for A-helix (1245−1240 cm^{-1}) to 1238−1236 cm^{-1} could indicate an A-like but not exactly A-helical geometry (*38*) of the phosphate backbone in the single-stranded RNA and its variants. The peak at 1218 cm^{-1} may have overlapping contributions of ribose sugars and mixed B-like helical conformation in the deoxy variants. In the case of ss7DNA (Figure 5a, vi), the dominant peak around 1221 cm^{-1} indicates a uniform B-like helical structure of the backbone even in DNA single strands.

In the spectra of RNA duplexes (ds7RNA and its deoxy variants, Figure 5b, i−v), two bands appear. The one at 1241 cm^{-1} is the characteristic marker band for A-form backbone geometry, while the other around 1221 cm^{-1} is assigned to the vibrations of the ribose sugar. The spectrum of double-stranded DNA (ds7DNA) shows only one broad band around 1222 cm^{-1}. This is the characteristic marker band for the B-helical backbone, which in this case has no contributions from the ribose sugar.

The antisymmetric PO_2^- stretching bands of ss7RNA and ss7DNA were compared with their corresponding complementary single strands (Supporting Information). In contrast to the antisymmetric PO_2^- stretching band of ss7RNA, the 1238 cm^{-1} peak in the ss7RNAcomp spectrum is less pronounced than the 1220 cm^{-1} peak (Supporting Information, Figure 1a ii). On the other hand, the antisymmetric PO_2^- stretching band of ss7DNAcomp (Supporting Information, Figure 1b ii) is similar to that of ss7DNA, both showing a broad band with a maximum around 1221 cm^{-1}.

The symmetric PO_2^- stretching mode which appears around 1090−1080 cm^{-1} shows a large decrease in band intensity for the single-stranded deoxy variants as compared to both ss7RNA and ss7DNA (Figure 6a). This occurs in both H_2O and D_2O buffer and is quantitatively reproducible. One possible explanation for the decrease in band intensity in the deoxy variants is that the vibrational coupling between the PO_2^- and the C−O stretching mode could be altered due to an increased heterogeneity in the backbone conformation on 2′-H substitution (*39*). In the duplexes, there is also a decrease in band intensity but not as large as in the single strands (Figure 6b).

(d) Furanose Frequency Region (1000−800 cm^{-1}). In the spectral region between 1000 and 800 cm^{-1}, absorption bands due to sugar ring vibrations appear which are markers for

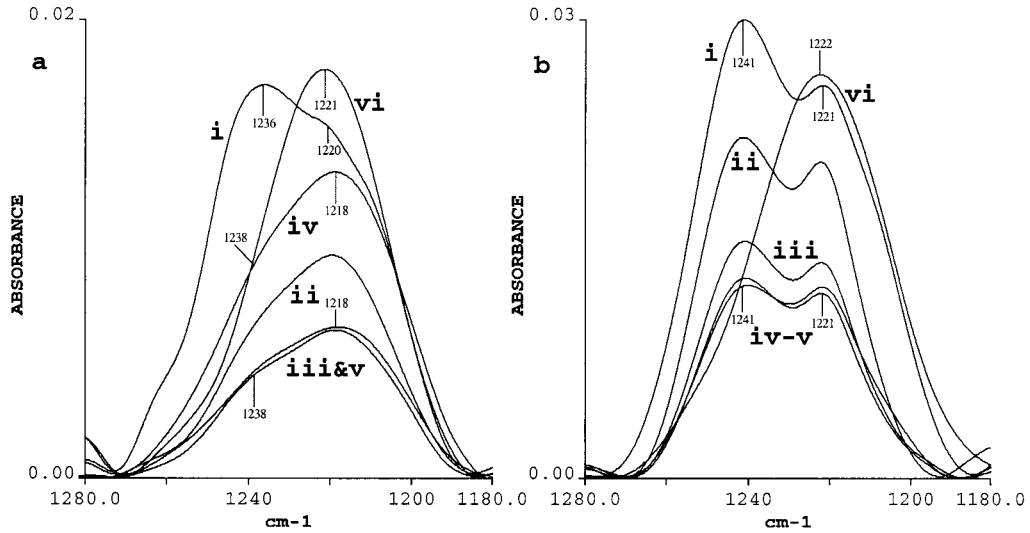

FIGURE 5: (a) FTIR spectra showing the 1280−1180 cm^{-1} region of single-stranded 7-mer sequences: (i) ss7RNA, (ii) ssdG451, (iii) ssdU452, (iv) ssdU453, (v) ssdC454, and (vi) ss7DNA. (b) FTIR spectra of double-stranded 7-mer sequences in the same spectral region: (i) ds7RNA, (ii) dsdG451, (iii) dsdU452, (iv) dsdU453, (v) dsdC454, and (vi) ds7DNA. All spectra recorded in H_2O at room temperature in 10 mM sodium cacodylate, 0.1 mM EDTA, pH 7.0, with a magnesium content of 10 Mg^{2+}/single strand and 20 Mg^{2+}/double strand.

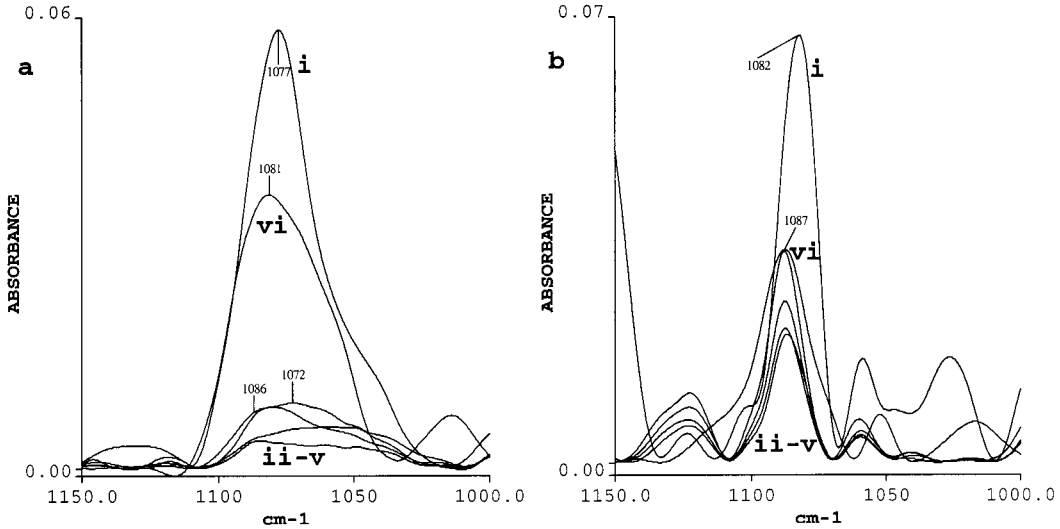

FIGURE 6: (a) FTIR spectra showing the 1150−1000 cm^{-1} region of single-stranded 7-mer sequences: (i) ss7RNA, (ii) ssdG451, (iii) ssdU452, (iv) ssdU453, (v) ssdC454, and (vi) ss7DNA. (b) FTIR spectra of double-stranded 7-mer sequences: (i) ds7RNA, (ii) dsdG451, (iii) dsdU452, (iv) dsdU453, (v) dsdC454, and (vi) ds7DNA. All spectra recorded in H_2O at room temperature in 10 mM sodium cacodylate, 0.1 mM EDTA, pH 7.0, with a magnesium content of 10 Mg^{2+}/single strand and 20 Mg^{2+}/double strand.

sugar conformation. The bands in the region 885−875, 865−860, and 815−800 cm^{-1} are markers for C3′-endo/anti or N-type sugar pucker found mostly in A-form helices. The band around 840−830 cm^{-1} is a marker for the C2′-endo/anti or S-type sugar pucker, found mostly in B-form helices (*38*, *40*−*44*). Figure 7 shows the sugar frequency region of the spectra of single strands and duplexes recorded in D_2O buffer. The changes in the spectral profile in this region should only be due to changes in sugar conformation. The single-stranded RNA (ss7RNA) spectrum shows a very broad band around 871 and 828 cm^{-1} (Figure 7a, i). The 871 cm^{-1} band indicates the presence of N-type sugar. On the other hand, the high wavenumber shift of the broad band around 828 cm^{-1}, compared to the marker bands for N-type sugar in this region, could reflect overlapping contributions of S-type sugar marker bands that occur in the region of 840−830 cm^{-1}. The presence of marker bands for both N- and S-type sugars in the ss7RNA spectra suggests that single-stranded RNA has heterogeneous sugar pucker. The single-stranded DNA, ss7DNA (Figure 7a, vi), on the other hand, shows one clear band at 832 cm^{-1}, a marker for S-type sugar, while no marker bands for N-type sugar in the regions 885−875, 865−860, and 815−800 cm^{-1} are seen.

In the single-stranded deoxy variants, marker bands for both N- and S-type sugar are seen (Figure 7a, ii−v). The exact peak positions are determined from second-derivative spectra. The broad band around 825 cm^{-1} in the spectrum of ssdU452 is composed two bands, one at 835 cm^{-1} and the other at 816 cm^{-1}, which are markers for S- and N-type pucker, respectively (Figure 7a, iii). Additional marker bands for N-type sugar are seen at 880 and 865 cm^{-1}. In all the other single-stranded deoxy variants, the broad band centered around 828 cm^{-1} (Figure 7a) is composed of bands that are markers for both N-type and S-type sugars. The changing shape of this band as the position of 2′-H substitution is varied indicates that the relative contributions of N- and

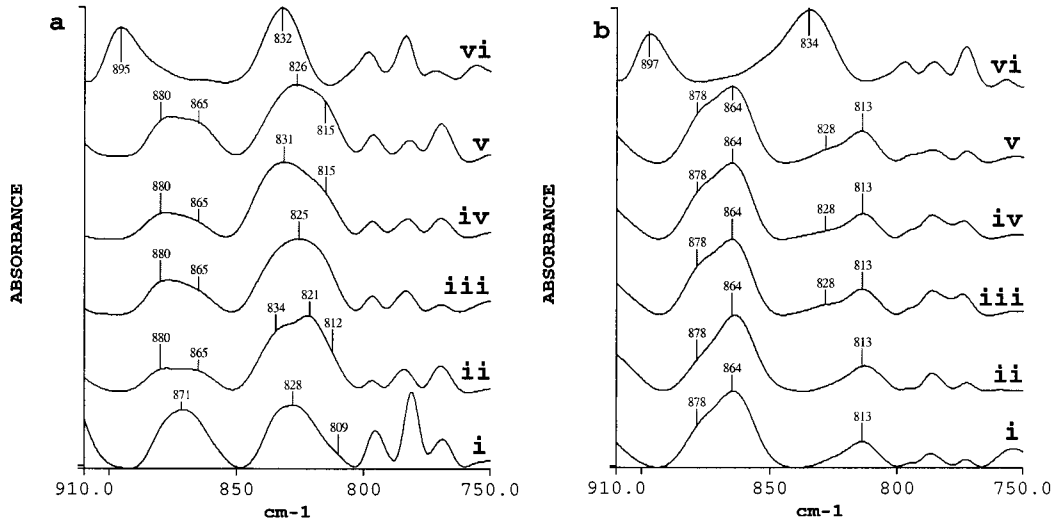

FIGURE 7: (a) Stacked FTIR spectra of the 910−750 cm^{-1} region of single-stranded 7-mer sequences: (i) ss7RNA, (ii) ssdG451, (iii) ssdU452, (iv) ssdU453, (v) ssdC454, and (vi) ss7DNA. (b) FTIR spectra of double-stranded 7-mer sequences: (i) ds7RNA, (ii) dsdG451, (iii) dsdU452, (iv) dsdU453, (v) dsdC454, and (vi) ds7DNA. All spectra recorded in D_2O at room temperature in 10 mM sodium cacodylate, 0.1 mM EDTA, pH 7.0, with a magnesium content of 10 Mg^{2+}/single strand and 20 Mg^{2+}/double strand.

S-type sugars changes with the position of the deoxyribose substitution.

In the duplexes (Figure 7b), the sugar pucker shows more uniformity than in the single strands. Clear marker bands of N-type sugar at 878, 864, and 813 cm^{-1} are seen in the spectrum of the duplex ds7RNA (Figure 7b, i). The absence of the 834 cm^{-1} band shows that for ds7RNA the riboses are in an N-type conformation characteristic of an A-helix backbone. The duplex DNA, ds7DNA, shows only the marker band for S-type sugar at 834 cm^{-1}, characteristic of a B-helical geometry. A 2′-H substitution in the sugar attached to the G451 does not change the spectra significantly (Figure 7b, ii). However, a 2′-H substitution in the sugar attached to either of the nucleotide residues 452−454 (dsdU452, dsdU453, and dsdC454) results in the appearance of a shoulder around 828 cm^{-1} beside the marker bands for the N-type sugar at 878, 864, and 813 cm^{-1}. This suggests the presence of some S-type sugar in dsdU452, dsdU453, and dsdC454 (Figure 7b, iii−v). This difference either could be dependent on the nature of the base in the nucleotide or can be a sequence position dependent effect in the short oligonucleotide. However, at this stage, one cannot rule out the presence of other types of sugar puckering besides N- and S-type in the single-stranded RNA. For the double-stranded deoxy variants, introduction of a deoxyribose sugar apparently has a much less perturbing effect on the duplex structure than in the single strands.

DISCUSSION

In this study we have demonstrated how a single deoxyribose (2′-OH→2′-H) substitution in the sugar−phosphate backbone of an RNA molecule can perturb both single-stranded and double-helical structures of a short mixed RNA sequence. Different optical spectroscopic techniques have been combined to highlight even small perturbations in the structures.

UV absorption results show that single-stranded RNA (ss7RNA) and DNA (ss7DNA) in general have less base stacking than their corresponding duplexes (ds7RNA and ds7DNA), as indicated by their lower hypochromicity values. For RNA double helices, a single 2′-H substitution in one strand results in a minor thermal destabilization of the double helix as compared to the all-ribose ds7RNA. The CD spectra (Figure 2) show that a 2′-H substitution has a more pronounced effect on the single-stranded RNA backbone than on the backbone of an RNA duplex. There is also a clear positional effect of this substitution in the single strands, where peak positions and crossover points in the CD spectra are affected by the position of the 2′-H substitution (Figure 2a).

In this study we show that it is possible to effectively use FTIR band assignments of longer repetitive sequences to characterize structural changes observed in short stretches of a mixed sequence of RNA and DNA. Bands observed in the base frequency region clearly show that the single-stranded RNA, DNA, and RNA deoxy variants were not in any associated form under the experimental conditions studied, while the corresponding double strand mixtures all formed double-helical structures (Figure 3).

The doublet in the region 1600−1550 cm^{-1}, that arises mainly due to C═N stretching vibrations of guanines, is sensitive to the environment of the guanines. A shift in this band position in ss7DNA as compared to ss7RNA indicates that despite similar base sequences (except that T replaces U in the DNA), the two guanine residues have a quite different environment and/or stacking interaction in the RNA as compared to the DNA single strand (Figure 3). A single deoxyribose substitution in the single-stranded RNA backbone alters the position and profile of this guanine-derived band irrespectively of whether the 2′-H substitution is made in a sugar attached to a guanine residue (ssdG451) or three nucleotides away from it (ssdC454). This suggests that in this short single-stranded RNA sequence, a structural perturbation due to a single 2′-H substitution can spread over the RNA backbone as far as three nucleotides away. For the double-helical RNA, a 2′-H substitution at any position in one strand of the duplex hardly affects this guanine doublet. The presence of a base-paired second strand in the duplex apparently imposes conformational restrictions that decrease

the perturbing effects of 2′-H substitution in the RNA backbone.

The 1500−1470 cm^{-1} band (Figure 4), assigned mainly to imidazolic ring vibrations of purines involving N7C8H bending vibration, is sensitive to any interaction at the N7 sites. The ss7RNA has two bands in this region, at 1489 and 1479 cm^{-1}, whose intensity ratio changes depending on the position of the 2′-H substitution in the single-stranded RNA deoxy variants. This change in band ratio indicates that the conformation of the single-stranded RNA changes with the position of the 2′-H substitution. This in turn may alter the interaction of the purine N7 sites with the solvent, which manifests in the changing band ratio with position of the 2′-H substitution. The single broad band at 1488 cm^{-1} seen in the spectrum of ss7DNA could be an indication of a more homogeneous environment for the purine N7 sites in this single-stranded DNA backbone.

The antisymmetric PO_2^- stretching mode in the region 1250−1200 cm^{-1} (Figure 5) is a sensitive marker band for conformational changes in the phosphate backbone. It acts as a reporter independent of the bases and the sugars, allowing one to view only the changes in the phosphate backbone. The position and profile of this band in these mixed-sequence single-stranded RNA, DNA, and RNA deoxy variants show that both RNA and DNA single strands are preorganized into A- and B-like helical conformations, respectively. The single-stranded DNA shows less heterogeneity in the backbone conformation than the RNA. This is consistent with the inference drawn from the behavior of the N7 bending vibration of the purines. The double-stranded RNA and all its deoxy variants adopt an A-helical geometry, whereas the ds7DNA adopts the expected B-helical geometry. Every RNA variant contains only one deoxyribose sugar, so the ribose contribution is similar when comparing all single- and all double-stranded deoxy variants. Hence, the change in ratio of the A- and B-form marker bands observed in this spectral region in the series of single-stranded (Figure 5a) and double-stranded deoxy variants (Figure 5b) could indicate the extent of a spreading B-like character in the variants. Interestingly, the antisymmetric PO_2^- stretching band has a different profile in the ss7RNA spectrum compared with that of ss7RNAcomp (Supporting Information, Figure 1a), whereas this band has quite similar profiles in the case of ss7DNA and ss7DNAcomp (Supporting Information, Figure 1b). This suggests that the backbone conformation of a short RNA single strand is relatively more sensitive to changes in the base sequence than its corresponding DNA counterpart. The symmetric PO_2^- stretching mode which appears around 1090−1080 cm^{-1} (Figure 6) also reflects the increased heterogeneity in the RNA single strands with 2′-H substitution, resulting in broadening and decrease in intensity of this band.

The changes that occur in the sugar conformation with 2′-H substitution are best reflected by the changes in the IR bands appearing in the furanose frequency region 1000−800 cm^{-1} (Figure 7). The appearance of characteristic marker bands for N-type and S-type sugar in the ss7RNA spectra shows that for this short single-stranded RNA in solution there exists heterogeneity in sugar conformations. In contrast, single-stranded DNA has a more uniform sugar pucker and is mostly in the S-type conformation characteristic of a B-helix. The results indicate that this particular sequence of single-stranded DNA is more preorganized into a B-like helical conformation even when the sugar pucker is concerned, as compared to the preorganization of the single-stranded RNA toward an A-helical conformation. The changes in intensity of the N- and S-marker bands show that a 2′-H substitution affects the neighboring sugar puckers, particularly in the single strands. This effect is dependent upon the position of the substitution in the single-stranded oligomer.

Concluding Remarks. There are very few spectroscopic studies devoted to short single-stranded RNA and DNA oligomers of mixed sequence. The results show that both RNA and DNA single strands have preorganized structures, with DNA showing a relatively uniform B-helical conformation at all levels, i.e., in the base, sugar, and phosphate backbone conformations. This is consistent with the recent work of Holbrook et al. (*45*) where they showed that disordered DNA single strands preorganize into single helices involving only intrastrand (vertical) interactions between neighboring bases, before the formation of double helices by association (docking) of single-helical strands. On the other hand, the single-stranded RNA is also preorganized into an A-like backbone conformation, but is more heterogeneous than its DNA counterpart. A single 2′-H substitution perturbs the single-stranded structures at all levels, of which the nature and extent are dependent on the position of the substitution in the strand. One should therefore be cautious in interpreting the results of experiments where 2′-H substitution is made to evaluate the role of 2′-OH groups in different RNA functions including catalysis, in particular if such substitution is made in presumably single-stranded RNA sequences. Any effect on RNA function cannot be unambiguously assigned to the absence of a 2′-OH group only, since such a substitution may perturb the local conformation to such an extent that a crucial RNA−RNA interaction might be significantly weakened. The presence of a base-paired second strand in a double helix imposes some restriction on the structural perturbation caused by a 2′-H substitution. Also the backbone conformation of single-stranded RNA is more sensitive to changes in base sequence than the DNA. All these results imply that a correct RNA−RNA contact requires fine-tuning of the role of the base sequence, the sugars, and the phosphate backbone conformation. In a recent work, Silverman and Cech (*46*) showed that the effect of 2′-H substitution in a ribose zipper motif in the P4−P6 domain of the *Tetrahymena* group I intron results only in local effects of hydrogen bond deletion with little evidence of context effects. However, as mentioned by them, the generality of their conclusions requires further experimentation, especially when 2′-OH-mediated interactions in other RNA motifs are considered. Our results provide further information on the effect of 2′-H substitution in RNA structures.

ACKNOWLEDGMENT

We thank Prof. Dr. Hartmut Fritzsche and Dr. Utz Dornberger for their invaluable assistance in FTIR handling and for very helpful discussions in the field of FTIR on nucleic acids.

SUPPORTING INFORMATION AVAILABLE

One FTIR figure is available as Supporting Information, showing the effects of base sequence in single-stranded RNA

on the phosphate backbone. This material is available free of charge via the Internet at http://pubs.asc.org.

REFERENCES

1. Egli, M., Portmann, S., and Usman, N. (1996) *Biochemistry 35*, 8489−8494.
2. Cheatham, T. E., and Kollman, P. A. (1997) *J. Am. Chem. Soc. 119*, 4805−4825.
3. Thibaudeau, C., Plavec, J., Garg, N., Papchikhin, A., and Chattopadhyaya, J. (1994) *J. Am. Chem. Soc. 116*, 4038−4043.
4. Plavec, J., Thibaudeau, C., and Chattopadhyaya, J. (1994) *J. Am. Chem. Soc. 116*, 6558−6560.
5. Wyatt, J. R., and Tinoco, I., Jr. (1993) in *The RNA World* (Gesteland, R. F., and Atkins, J. F., Eds.) pp 465−496, Cold Spring Harbor Laboratory Press, Cold Spring Harbor, NY.
6. Holbrook, S. R. (1998) in *RNA Structure and Function* (Simons, R. W., and Grunberg-Manago, M., Eds.) pp 147−174, Cold Spring Harbor Laboratory Press, Cold Spring Harbor, NY.
7. Ban, C., Ramakrishnan, B., and Sundaralingam, M. (1994) *J. Mol. Biol. 236*, 275−285.
8. Egli, M., Usman, N., and Rich, A. (1993) *Biochemistry 32*, 3221−3237.
9. Perreault, J. P., Labuda, D., Usman, N., Yang, J. H., and Cedergren, R. (1991) *Biochemistry 30*, 4020−4025.
10. Chowrira, B. M., Berzalherranz, A., Keller, C. F., and Burke, J. M. (1993) *J. Biol. Chem. 268*, 19458−19462.
11. Loria, A., and Pan, T. (1997) *Biochemistry 36*, 6317−6325.
12. Bevilacqua, P. C., and Turner, D. H. (1991) *Biochemistry 30*, 10632−10640.
13. Pyle, A. M., and Cech, T. R. (1991) *Nature 350*, 628−631.
14. Herschlag, D., Eckstein, F., and Cech, T. R. (1993) *Biochemistry 32*, 8299−8311.
15. Strobel, S. A., and Cech, T. R. (1993) *Biochemistry 32*, 13593−13604.
16. Narlikar, G. J., Khosla, M., Usman, N., and Herschlag, D. (1997) *Biochemistry 36*, 2465−2477.
17. Whoriskey, S. K., Usman, N., and Szostak, J. W. (1995) *Proc. Natl. Acad. Sci. U.S.A. 92*, 2465−2469.
18. Michel, F., and Westhof, E. (1990) *J. Mol. Biol. 216*, 585−610.
19. Sarkar, M., Sigurdsson, S., Tomac, S., Sen, S., Rozners, E., Sjöberg, B. M., Strömberg, R., and Gräslund, A. (1996) *Biochemistry 35*, 4678−4688.
20. Sarkar, M., Dornberger, U., Rozners, E., Fritzsche, H., Strömberg, R., and Gräslund, A. (1997) *Biochemistry 36*, 15463−15471.
21. Strömberg, R., and Stawinski, J. (1999) in *Current Protocols in Nucleic Acid Chemistry* (Beaucage, S., Ed.) Unit 3.4, Wiley, New York (in press).
22. Mccollum, C., and Andrus, A. (1991) *Tetrahedron Lett. 32*, 4069−4072.
23. Puglisi, J. D., and Tinoco, I., Jr. (1989) *Methods Enzymol. 180*, 304−325.
24. Johnson, W. C., Jr. (1985) *Methods Biochem. Anal. 31*, 61−163.
25. Gray, D. M., Ratliff, R. L., and Vaughan, M. R. (1992) *Methods Enzymol. 211*, 389−406.
26. Tsuboi, M. (1969) in *Applied Spectroscopy Reviews* (Brame, E. G. J., Ed.) Vol. 3, pp 45−90, Marcel Dekker, New York.
27. Dagneaux, C., Liquier, J., Scaria, P. V., Shafer, R. H., and Taillandier, E. (1994) in *Structural Biology: The State of Art, Proceedings of the VIIIth Conversion, State University of New York, Albany, New York, 1993* (Sarma, R. H., and Sarma, M. H., Eds.) pp 103−111, Adenine Press, Schenectady, NY.
28. Taboury, J. A., Liquier, J., and Taillandier, E. (1985) *Can. J. Chem. 63*, 1904−1909.
29. Dagneaux, C., Liquier, J., and Taillandier, E. (1995) *Biochemistry 34*, 14815−14818.
30. Abdelkafi, M., Leulliot, N., Baumruk, V., Bednarova, L., Turpin, P. Y., Namane, A., Gouyette, C., Huynh-Dinh, T., and Ghomi, M. (1998) *Biochemistry 37*, 7878−7884.
31. Taillandier, E., and Liquier, J. (1992) *Methods Enzymol. 211*, 307−335.
32. Mohammadi, S., Klement, R., Shchyolkina, A. K., Liquier, J., Jovin, T. M., and Taillandier, E. (1998) *Biochemistry 37*, 16529−16537.
33. Letellier, R., Ghomi, M., and Taillandier, E. (1986) *J. Biomol. Struct. Dyn. 3*, 671−687.
34. Letellier, R., Ghomi, M., and Taillandier, E. (1987) *J. Biomol. Struct. Dyn. 4*, 663−683.
35. White, A. P., and Powell, J. W. (1995) *Biochemistry 34*, 1137−1142.
36. Dagneaux, C., Liquier, J., and Taillandier, E. (1995) *Biochemistry 34*, 16618−16623.
37. Liquier, J., Akhebat, A., Taillandier, E., Ceolin, F., Dinh, T. H., and Igolen, J. (1991) *Spectrochim. Acta, Part A: Mol. Biomol. Spectrosc. 47*, 177−186.
38. Taillandier, E., Ridoux, J. P., Liquier, J., Leupin, W., Denny, W. A., Wang, Y., Thomas, G. A., and Peticolas, W. L. (1987) *Biochemistry 26*, 3361−3368.
39. Guan, Y., and Thomas, G. J., Jr. (1996) *Biopolymers 39*, 813−835.
40. Dohy, D., Ghomi, M., and Taillandier, E. (1989) *J. Biomol. Struct. Dyn. 6*, 741−754.
41. Letellier, R., Ghomi, M., and Taillandier, E. (1989) *J. Biomol. Struct. Dyn. 6*, 755−768.
42. Liquiers, J., Taillandier, E., Peticolas, W. L., and Thomas, G. A. (1990) *J. Biomol. Struct. Dyn. 8*, 295−302.
43. Liquier, J., Coffinier, P., Firon, M., and Taillandier, E. (1991) *J. Biomol. Struct. Dyn. 9*, 437−445.
44. Ouali, M., Letellier, R., Sun, J. S., Akhebat, A., Adnet, F., Liquier, J., and Taillandier, E. (1993) *J. Am. Chem. Soc. 115*, 4264−4270.
45. Holbrook, J. A., Capp, M. W., Saecker, R. M., and Record, M. T., Jr. (1999) *Biochemistry 38*, 8409−8422.
46. Silverman, S. K., and Cech, T. R. (1999) *Biochemistry 38*, 8691−8702.

BI992055N